J|A|C|S
ARTICLES
Published on Web 04/17/2002

Femtosecond Electron-Transfer Reactions in Mono- and Polynucleotides and in DNA

Gavin D. Reid,*,† Douglas J. Whittaker,† Mark A. Day,† David A. Turton,† Veysel Kayser,† John M. Kelly,‡ and Godfrey S. Beddard†

Contribution from the School of Chemistry, University of Leeds, Leeds, LS2 9JT, U.K., and Department of Chemistry, University of Dublin, Trinity College, Dublin 2, Ireland

Received October 5, 2001

Abstract: Quenching of redox active, intercalating dyes by guanine bases in DNA can occur on a femtosecond time scale both in DNA and in nucleotide complexes. Notwithstanding the ultrafast rate coefficients, we find that a classical, nonadiabatic Marcus model for electron transfer explains the experimental observations, which allows us to estimate the electronic coupling (330 cm^{-1}) and reorganization (8070 cm^{-1}) energies involved for thionine-[poly(dG-dC)]$_2$ complexes. Making the simplifying assumption that other charged, π-stacked DNA intercalators also have approximately these same values, the electron-transfer rate coefficients as a function of the driving force, ΔG, are derived for similar molecules. The rate of electron transfer is found to be independent of the speed of molecular reorientation. Electron transfer to the thionine singlet excited state from DNA obtained from calf thymus, salmon testes, and the bacterium, micrococcus luteus (lysodeikticus) containing different fractions of G−C pairs, has also been studied. Using a Monte Carlo model for electron transfer in DNA and allowing for reaction of the dye with the nearest 10 bases in the chain, the distance dependence scaling parameter, β, is found to be 0.8 ± 0.1 $Å^{-1}$. The model also predicts the redox potential for guanine dimers, and we find this to be close to the value for isolated guanine bases. Additionally, we find that the pyrimidine bases are barriers to efficient electron transfer within the superexchange limit, and we also infer from this model that the electrons do not cross between strands on the picosecond time scale; that is, the electronic coupling occurs predominantly through the π-stack and is not increased substantially by the presence of hydrogen bonding within the duplex. We conclude that long-range electron transfer in DNA is not exceptionally fast as would be expected if DNA behaved as a "molecular wire" but nor is it as slow as is seen in proteins, which do not benefit from π-stacking.

Introduction

Ultrafast electron transfer involving DNA has recently received considerable attention both experimentally[1−4] and theoretically.[5−10] Electron transfer is important for DNA damage and repair,[11−13] and many applications in molecular electronics are envisaged.[14−17] In particular, ever since the first studies of charge transport in DNA,[18] there has been considerable debate as to whether electron transfer in a DNA environment is unexpectedly fast; for a recent review, see Barbara and Olson.[19] Photoinduced electron-transfer reactions can also lead to DNA damage, including adduct formation,[20] and such reactions might in the future be used for antitumor therapy.

The structure of B-form DNA determines the nature of the intervening medium between intercalated electron donors and acceptors within the ordered stack of planar purine and pyrimidine bases, which is surrounded by water-containing grooves and the charged sugar−phosphate backbone. In proteins, a balance of the interactions between polar and nonpolar residues

* To whom correspondence should be addressed. Tel: 44 113 233 6405. Fax: 44 113 233 6565. E-mail: g.d.reid@chem.leeds.ac.uk.
† University of Leeds.
‡ University of Dublin.

(1) Reid, G. D.; Whittaker, D. J.; Day, M. A.; Creely, C. M.; Tuite, E. M.; Kelly, J. M.; Beddard, G. S. *J. Am. Chem. Soc.* **2001**, *123*, 6953−6954.
(2) Wan, C.; Fiebig, T.; Schiemann, O.; Barton, J. K.; Zewail, A. H. *Proc. Natl. Acad. Sci. U.S.A.* **2000**, *97*, 14052−14055.
(3) Lewis, F. D.; Wu, T.; Liu, X.; Letsinger, R. L.; Greenfield, S. R.; Miller, S. E.; Wasielewski, M. R. *J. Am. Chem. Soc.* **2000**, *122*, 2889−2902.
(4) Kononov, A. I.; Moroshkina, E. B.; Tkachenko, N. V.; Lemmetyinen, H. *J. Phys. Chem. B* **2001**, *105*, 535−541.
(5) Porath, D.; Bezryadin, A.; De Vries, S.; Dekker, C. *Nature* **2000**, *403*, 635−638.
(6) Tavernier, H. L.; Fayer, M. D. *J. Phys. Chem. B* **2000**, *104*, 11541−11550.
(7) Schlag, E. W.; Yang, D. Y.; Sheu, S. Y.; Selzle, H. L.; Lin, S. H.; Rentzepis, P. M. *Proc. Natl. Acad. Sci. U.S.A.* **2000**, *97*, 9849−9854.
(8) Beratan, D. N.; Priyadarshy, S.; Risser, S. M. *Chem. Biol.* **1997**, *4*, 3−8.
(9) Giese, B.; Wessely, S.; Spormann, M.; Lindemann, U.; Meggers, E.; Michel-Beyerle, M. E. *Angew. Chem., Int. Ed.* **1999**, *38*, 996−998.
(10) Jortner, J.; Bixon, M.; Langenbacher, T.; Michel-Beyerle, M. E. *Proc. Natl. Acad. Sci. U.S.A.* **1998**, *95*, 12759−12765.
(11) Armitage, B. *Chem. Rev.* **1998**, *98*, 1171−1200.
(12) Burrows, C. J.; Muller, J. G. *Chem. Rev.* **1998**, *98*, 1109−1151.
(13) Schuster, G. B. *Acc. Chem. Res.* **2000**, *33*, 253−260.
(14) Fox, M. A. *Acc. Chem. Res.* **1999**, *32*, 201−207.
(15) Berlin, Y. A.; Burin, A. L.; Ratner, M. A. *Superlattices Microstruct.* **2000**, *28*, 241−252.
(16) Dekker, C.; Ratner, M. A. *Phys. World* **2001**, *14*, 29−33.
(17) Rinaldi, R.; Branca, E.; Cingolani, R.; Masiero, S.; Spada, G. P.; Gottarelli, G. *Appl. Phys. Lett.* **2001**, *78*, 3541−3543.
(18) Eley, D. D.; Spivey, D. I. *Trans. Faraday Soc.* **1962**, *58*, 411−415.
(19) Barbara, P. F.; Olson, E. J. C. In *Electron Transfer: From Isolated Molecules to Biomolecules, Part Two*; Jortner, J., Bixon, M., Eds.; John Wiley & Sons: New York, 1999; *Adv. Chem. Phys. 107*, pp 647−676.
(20) Jacquet, L.; Davies, R. J. H.; Kirsch-De Mesmaeker, A.; Kelly, J. M. *J. Am. Chem. Soc.* **1997**, *119*, 11763−11768.

10.1021/ja0172363 CCC: $22.00

both with themselves and with the solvent usually determines the secondary and tertiary structure, resulting in a very different medium for electron transfer. This difference in structure poses the question as to whether electron transfer in DNA behaves either in the same way as in proteins,[21] in well-defined donor−spacer−acceptor complexes,[22] or in neither.

The excited singlet states of the bases in DNA are extremely short-lived, that is, <1 ps,[23] and it has been suggested recently that this may play some part in protecting the molecule from photodamage by ultraviolet light. However, photodynamic degradation of DNA may also be induced by ultrafast redox reactions,[11−13] and here the phenothiazine family of dyes is important,[24] because the excited states of the dyes are strongly quenched when they bind near guanine bases.[1,25−27] Quenching by adenine should be far slower than by guanine, because the oxidation potential of adenine is higher, while quenching by the pyrimidine bases, which lie at still higher potential, is not observed; that is, $E°$ (G) < $E°$ (A) < $E°$ (C) ≈ $E°$ (T).[28,29] The possibility of proton-coupled, electron-transfer reactions has also been the subject of recent experimental and theoretical attention.[30−32]

The dependence of the rate of electron transfer as a function of ΔG has been studied extensively. While a quantum-mechanical model is often necessary, particularly in the "inverted" regime, at very short internuclear separation, or in the strong coupling limit,[33,34] the classical result due to Marcus[35] has explained the majority of experimental observations of biological electron transfer over as many as 10 orders of magnitude in rate coefficient.[36] Whether nonclassical effects, such as those produced by delocalization of charge along the base π-stack in DNA, by strong adiabatic electronic coupling between electron donor and acceptor or coupling of the reaction coordinate to high frequency, intramolecular vibrational modes need to be invoked, are the points we address in this work.

The rate coefficient, k_0, for nonadiabatic electron transfer is given by

$$k_0 = \frac{2\pi|V_0|^2}{\hbar} F(\Delta G,\lambda)$$

where V_0 is the electronic coupling matrix element, and F is the thermally averaged, Franck−Condon weighted density of states. The expected distance dependence of k_0 depends on the overlap of the relevant wave functions and so falls off exponentially with the separation of donor and acceptor $|V|^2 = |V_0|^2 \exp(-\beta(r - r_0))$, where β is a scaling parameter and r the internuclear separation, r_o being the distance of closest approach. Therefore, experimentally, the rate coefficient of interest, k, is given by $k = k_0 \exp(-\beta(r - r_0))$. If DNA behaves as a "molecular wire" and long-range electron transfer is particularly efficient, it has been proposed that $\beta \leq 0.2$ Å^{-1},[37] whereas if electron transfer is essentially the same as in a protein, β would be in the range 0.9 → 1.4 Å^{-1}.[21] It should be noted, however, that different and possibly competing mechanisms of charge separation might result from the use of different donors or acceptors. First, direct transfer between adjacent donor and acceptor will show the expected exponential distance dependence. If there are intervening base pairs, a two center, single-step superexchange model will also depend exponentially on distance[10] but with a different scaling parameter and will occur in competition with direct transfer. A charge-hopping mechanism[9,38,39] between intervening bases, with an apparently weak distance dependence, could also occur depending on the energy gaps between the low lying vibronic states of the initially excited molecule and the vibronic manifolds of the charge-separated species. Considering electron transfer through intervening bases, superexchange should dominate when the energy gap between the donor and the "bridging" states is $\gg k_B T$, while a hopping mechanism will prevail if the energies of the donor and of each of the intermediate states are approximately degenerate. In a hopping mechanism, spectral evidence for population of the intermediate states should be observable.

Experimentally, optical excitation of an intercalated dye is a good method by which electrons or holes can be rapidly injected into DNA strands.[1,27,40−42] Alternatively, covalently bound species have also been used to initiate photoinduced electron transfer within duplex DNA.[37,43−45] In particular, Lewis et al.[3] have covalently bound stilbenedicarboxamide to small, synthetic DNA hairpins and found β to be 0.7 Å^{-1} for the forward electron transfer and 0.9 Å^{-1} for the reverse step. It was suggested that these relatively small β might be due to the similarity in energy of the HOMO in stilbene to that in DNA. Jortner et al.[10] have studied these synthetic hairpins theoretically and support a superexchange mechanism for charge separation and an exponential distance dependence of the rate coefficient. In another study, Wan et al.[2] incorporated 2-aminopurine, an isomer of adenine, into well-characterized DNA assemblies, and a similar distance dependence to that of Lewis was observed, $\beta = 0.6$ Å^{-1}.

(21) Langen, R.; Colon, J. L.; Casimiro, D. R.; Karpishin, T. B.; Winkler, J. R.; Gray, H. B. *J. Biol. Inorg. Chem.* **1996**, *1*, 221.
(22) Harrison, R. J.; Pearce, B.; Beddard, G. S.; Cowan, J. A.; Sanders, J. K. M. *Chem. Phys.* **1987**, *116*, 429−448.
(23) Pecourt, J.-M. L.; Peon, J.; Kohler, B. *J. Am. Chem. Soc.* **2000**, *122*, 9348−9349.
(24) OhUigin, C.; McConnell, D. J.; Kelly, J. M.; Van der Putten, W. J. M. *Nucleic Acids Res.* **1987**, *15*, 7411−7427.
(25) Beddard, G. S.; Kelly, J. M.; Van der Putten, W. J. M. *J. Chem. Soc., Chem. Commun.* **1990**, 1346−1347.
(26) Kelly, J. M.; Tuite, E. M.; Van der Putten, W. J. M.; Beddard, G. S.; Reid, G. D. *NATO Adv. Study Inst. Ser., Ser. C* **1992**, *371*, 375−381.
(27) Tuite, E.; Kelly, J. M.; Beddard, G. S.; Reid, G. D. *Chem. Phys. Lett.* **1994**, *226*, 517−524.
(28) Seidel, C. A. M.; Schulz, A.; Sauer, M. H. M. *J. Phys. Chem.* **1996**, *100*, 5541−5553.
(29) Steenken, S.; Jovanovic, S. V. *J. Am. Chem. Soc.* **1997**, *119*, 617−618.
(30) Weatherly, S. C.; Yang, I. V.; Thorp, H. H. *J. Am. Chem. Soc.* **2001**, *123*, 1236−1237.
(31) Shafirovich, V.; Dourandin, A.; Luneva, N. P.; Geacintov, N. E. *J. Phys. Chem. B* **2000**, *104*, 137−139.
(32) Steenken, S. *Biol. Chem.* **1997**, *378*, 1293−1297.
(33) Wynne, K.; Reid, G. D.; Hochstrasser, R. M. *J. Chem. Phys.* **1996**, *105*, 2287−2297.
(34) Wynne, K.; Hochstrasser, R. M. In *Electron Transfer: From Isolated Molecules to Biomolecules, Part Two*; Jortner, J., Bixon, M., Eds.; John Wiley & Sons: New York, 1999; *Adv. Chem. Phys. 107*, pp 263−309.
(35) Marcus, R. A.; Sutin, N. *Biochim. Biophys. Acta* **1985**, *811*, 265−322.
(36) Page, C. C.; Moser, C. C.; Chen, X.; Dutton, P. L. *Nature* **1999**, *402*, 47−52.
(37) Murphy, C. J.; Arkin, M. R.; Jenkins, Y.; Ghatlia, N. D.; Bossmann, S. H.; Turro, N. J.; Barton, J. K. *Science* **1993**, *262*, 1025−1029.
(38) Berlin, Y. A.; Burin, A. L.; Ratner, M. A. *J. Am. Chem. Soc.* **2001**, *123*, 260−268.
(39) Bixon, M.; Jortner, J. *J. Phys. Chem. A* **2001**, *105*, 10322−10328.
(40) Brun, A. M.; Harriman, A. *J. Am. Chem. Soc.* **1992**, *114*, 3656−3660.
(41) Arkin, M. R.; Stemp, E. D. A.; Holmlin, R. E.; Barton, J. K.; Hormann, A.; Olson, E. J. C.; Barbara, P. F. *Science* **1996**, *273*, 475−480.
(42) Lincoln, P.; Tuite, E.; Norden, B. *J. Am. Chem. Soc.* **1997**, *119*, 1454−1455.
(43) Kelley, S. O.; Holmlin, R. E.; Stemp, E. D. A.; Barton, J. K. *J. Am. Chem. Soc.* **1997**, *119*, 9861−9870.
(44) Kelley, S. O.; Barton, J. K. *Science* **1999**, *283*, 375−381.
(45) Fukui, K.; Tanaka, K. *Angew. Chem., Int. Ed.* **1998**, *37*, 158−161.

Table 1. Redox Active, Blue Dyes Showing Their Reduction Potentials, E^0, Relative to NHE and the Energy of the Singlet States, E_{0-0}

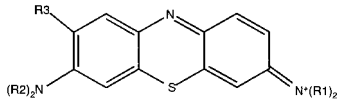

Thionine, Th: R1 = R2 = R3 = H.

Methylene Blue, MB: R1 = R2 = CH_3 R3 = H

Toluidine Blue, Tolb: R1 = R3 = CH_3 R2 = H

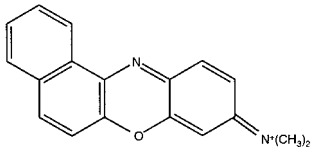

Meldola's Blue, Melb

dye	E^0/eV	E_{0-0}/eV
thionine	−0.03[48]	2.03
methylene blue	−0.09[27]	1.83
toluidine blue	−0.04[49]	1.88
Meldola's blue	−0.04[49]	2.03

Recently, in a study of the ultrafast electron-transfer reactions between thionine, Th (3,7-diaminophenazathionium chloride), and guanine, G, bases in guanosine-5′-monophosphate, GMP, and poly(dG-dC)·poly(dG-dC), $[poly(dG\text{-}dC)]_2$, which forms a B-DNA structure, we found both the forward and the reverse reaction rates, k_f and k_r, to be on the femtosecond time scale, more than 10 times faster than rotational motion.[1] We showed also that it was not a small subset of excited molecules that reacted on this time scale, and we explained these measurements of k_f and k_r using a classical Marcus model despite the ultrafast time scale of the reaction. The reaction scheme is

$$Th^+{:}G \xrightarrow{h\nu} Th^+{*}{:}G \xrightarrow{k_f} [Th^{\bullet}{:}G^{\bullet+}] \xrightarrow{k_r} Th^+{:}G \qquad (1)$$

In the present work, we have studied a range of intercalating dyes, thionine, toluidine blue, Tolb (3-Amino-7-(dimethylamino)-2-methylphenazathionium chloride), and Meldola's blue, Melb (7-(dimethylamino)-1,2-benzophenoxazine), of similar chemical structure and redox potential (Table 1). We have extended our experiments to reactions of thionine with 2′-deoxyadenosine-5′-monophosphate, dAMP, and poly(dA-dT)·poly(dA-dT), $[poly(dA\text{-}dT)]_2$, and to Meldola's blue and toluidine blue with GMP. We show for the first time that thionine is quenched by DNA over a range of time scales that depends on the ratio of G−C to A−T pairs in a manner that is not a simple sum of guanine and adenine quenching rates to nearest neighbors. We have used three native DNAs, from calf thymus (ct) and salmon testes (st), both composed of similar guanine-to-adenine ratios (quoted as 42% and 41.2% G−C, respectively) and from the bacterium micrococcus luteus (mc), which contains a significantly larger proportion of guanine (72% G−C). The dyes were chosen in the expectation that they should react with guanine bases on the femtosecond to picosecond time scale. Quenching of the dyes is due to electron transfer from the base to the dye excited singlet state. The single-electron oxidation potential of guanine was thought to depend strongly on its neighboring bases,[12,46,47] and, therefore, a distribution of electron-transfer rates within DNA might be expected. However, measurements near or at the peak of the Marcus curve, where the rate coefficient is relatively independent of changes in ΔG, allow us to make much safer predictions of the electronic coupling and reorganization energies.

Experimental Section

Solutions of dye (50 μM, Aldrich) in 5 mM phosphate buffer (pH = 6.9) containing either $[poly(dA\text{-}dT)]_2$, $[poly(dG\text{-}dC)]_2$ (1.5 mM nucleotide), GMP, dAMP (100 mM), or DNA (7mM nucleotide) were studied. Dyes were purified on neutral alumina, recrystallized three times from ethanol, and dried under vacuum. The purity was confirmed by NMR and visible absorption and emission spectroscopies. The nucleotides and DNAs were used as supplied (Sigma). Binding studies[50] on thionine with the mono- and polynucleotides and with DNA show that a very high fraction of the dye is bound. Binding constants are >900 M^{-1} for mononucleotides and 10^6 M^{-1} to polynucleotides and DNA. There appears to be no particular preference for G−C rather than A−T binding. Also, there was no spectroscopic evidence for dimers of the dye, which can occur at these concentrations in the absence of nucleotide. 1:2 complexes are expected to predominate for mononucleotides, and, under conditions of low ionic strength, binding to the synthetic polynucleotides and to DNA is predominantly intercalative.[50,51] The nucleotide-to-dye ratio in the polymers was in excess of 30:1 in all cases and higher still for the DNAs to further favor intercalative binding.

Our femtosecond laser and transient absorption spectrometer is entirely home-built and has not been described in detail elsewhere. It consists of a Kerr-lens mode-locked, Ti:sapphire oscillator producing 13 fs pulses at 800 nm, pumped by 6.5 W from an all-lines, continuous argon ion laser (Coherent Innova 310). These pulses are temporally stretched and amplified in a regenerative amplifier pumped by an intracavity doubled, 2.9 kHz acousto-optically Q-switched (QS27-4SN, Gooch & Housego Ltd.), Nd:YAG laser. The pumping chamber (Spectron Laser Systems 902TQ) contains a 100 mm long, flash-lamp pumped rod, relay imaged onto a coated (DBAR/1064+532/PVD/C) 4 × 4 × 7 mm^3 KTP crystal (Cristal Laser SA) in a *z*-folded configuration. The laser produces two beams of 8.5 W each at 532 nm when driven at a lamp current of only 14 A, limited by damage to the KTP at this repetition rate.

The regenerative amplifier is a three-mirror cavity containing a fast Pockels cell (Medox Electrooptics) to inject and dump the pulses and a 20 mm Ti:sapphire rod doped to absorb ca. 90% of the pump light. The pulses from the regenerative amplifier (300 μJ) are compressed to 30−40 fs (limited by gain narrowing, not spectral dispersion) with an ultimate energy of 150 μJ/pulse. A combination of high refractive index prisms (SF10) and unequal groove density diffraction gratings in the stretcher (1200 L mm^{-1}) and compressor (1600 L mm^{-1}) allows the correction of all phase terms up to and including fourth order.[52]

To allow for tuneability of pump and probe wavelengths through most of the visible spectrum, we have constructed two independent, noncollinear, optical parametric amplifiers (NOPAs) as pump and probe sources. A seed pulse, which is a single filament "continuum" of white light generated in a 1 mm path of sapphire, is amplified by the frequency doubled (in 1 mm LBO) output of the amplifier (10 μJ), in a noncollinear arrangement using type I BBO (2 mm, $\theta = 32°$, $\varphi = 90°$, AR@400 nm + HT@500−2400 nm, Ingcrys Laser Systems). The pump beam generates a cone of parametric superfluorescence from the BBO crystal. The crystal angle is adjusted such that the superfluor-

(46) Saito, I.; Takayama, M.; Sugiyama, H.; Nakatani, K. *J. Am. Chem. Soc.* **1995**, *117*, 6406−6407.
(47) Sugiyama, H.; Saito, I. *J. Am. Chem. Soc.* **1996**, *118*, 7063−7068.
(48) Guha, S. N.; Moorthy, P. N.; Kishore, K.; Naik, D. B.; Rao, K. N. *Proc.-Indian Acad. Sci., Chem. Sci.* **1987**, *99*, 261−271.
(49) Lobo, M. J.; Miranda, A. J.; Tunon, P. *Electroanalysis* **1997**, *9*, 191−202.
(50) Tuite, E.; Kelly, J. M. *Biopolymers* **1995**, *35*, 419−433.
(51) Rohs, R.; Sklenar, H.; Lavery, R.; Roeder, B. *J. Am. Chem. Soc.* **2000**, *122*, 2860−2866.
(52) Reid, G. D.; Wynne, K. In *Encyclopedia of Analytical Chemistry*; Meyers, R. A., Ed.; John Wiley & Sons: Chichester, 2000; pp 13644−13670.

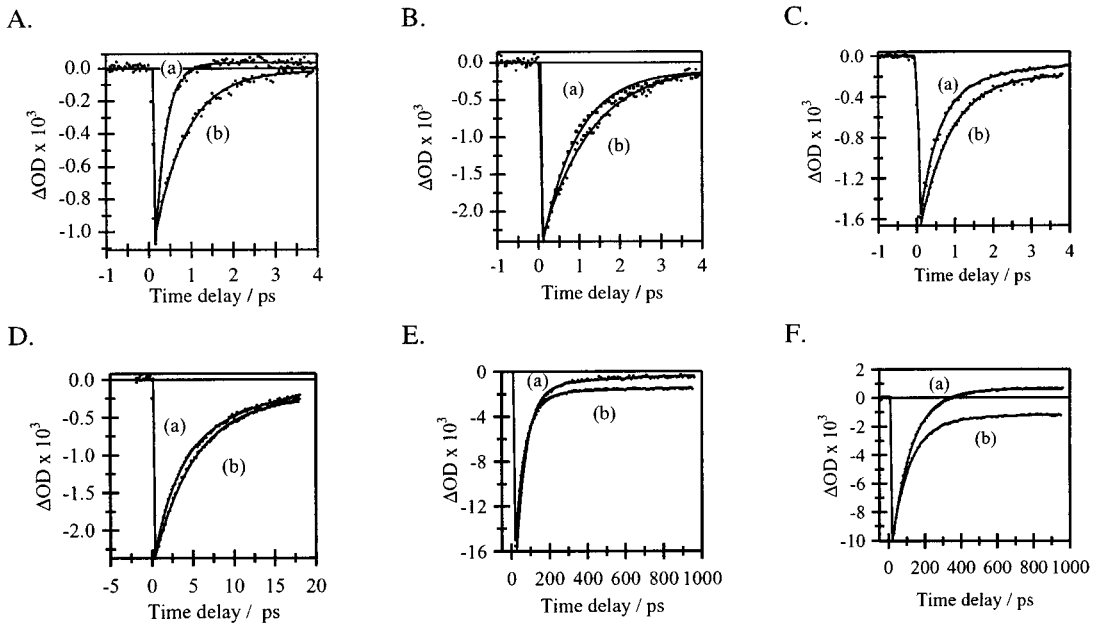

Figure 1. (A) Thionine-[poly(dG-dC)]$_2$. (B) Thionine-GMP. (C) Meldola's blue-GMP. (D) Toluidine blue-GMP (note time scale). (E) Thionine-AMP (note time scale). (F) Thionine-[poly(dA-dT)]$_2$. In each plot (a) is the gain signal (670 or 710 nm) and (b) the ground-state recovery (600 nm). We believe that the oxidized bases contribute to the long-time absorption signal in Figure A(a) and F(a), i.e., when in the B-DNA type environment. The residual bleach in the gain signals, B(a) through E(a), is a result of a small overlap of the absorption and emission spectra.

escence shows no spatial dispersion. By directing the continuum beam along the cone axis, a large spectral bandwidth from the white light can be phase matched simultaneously.[53] Tuning the relative delay between pump and seed and controlling the chirp on the seed pulse change the center wavelength and bandwidth of the amplified light. The result after compression, using a pair of BK7 prisms, is ultrashort visible pulses tuneable continuously from ca. 480 to 750 nm with a duration of 10 to 30 fs depending on wavelength.

Samples in a 1 mm path length cuvette were excited with 25 fs, ≤200 nJ pulses of 600 nm light from one optical parametric amplifier, focused to a diameter of 100 μm. The pump beam was chopped synchronously (New Focus 3501) at half of the repetition rate of the amplifier. The transient species so-formed were monitored using pulses from the second parametric amplifier, also with 25 fs resolution, either at 600 nm to observe the ground state recovery, or at 670 nm to record the loss of the excited state by the decay of the stimulated emission (gain) signal. Both the central wavelength and the bandwidth of the pump and probe beams were measured routinely using a spectrograph and CCD camera. The relative polarization of the pump and probe was set either to 54.7° ("magic angle"), to remove any contributions from orientational effects, or to 0° (parallel) and 90° (orthogonal) for anisotropy measurements by the rotation of a half-waveplate in the pump beam. The anisotropy, $r(t)$, is calculated from $r(t) = [I_{||}(t) - I_{\perp}(t)]/[I_{||}(t) + 2I_{\perp}(t)]$.

The probe beam was split into two parts and the intensities measured on a pair of large-area photodiodes (New Focus 2031) interfaced to a PC, to record the difference in absorbance (ΔOD) between the excited and ground-state species as a function of the relative pump−probe delay. A ΔOD of $\leq 10^{-4}$ could be measured by averaging for 1 s at each time delay. Typically, 20−60 scans were averaged to remove long-time drifts in pump energy. We estimate the error on the measured lifetimes to be ±5%.

The stimulated emission decay rates were confirmed where possible by fluorescence measurements using time-correlated, single photon counting (TCSPC). The laser source was a cw-modelocked, Nd:YAG laser (Spectron Laser Systems), synchronously pumping a cavity-dumped dye laser. Fluorescence decays were recorded with 40 ps resolution using a microchannel plate photomultiplier tube (Hamamatsu) connected to a computer board containing the fast digitization electronics (Becker and Hickl SPC-630).

Results

1. Mono- and Polynucleotides. For each of the dye-nucleotide or dye-DNA complexes, the excited-state decay has been monitored through its stimulated emission after excitation with 25 fs, 600 nm pulses. To observe this signal, we have selected wavelengths where there is little or no transient absorption or ground-state bleaching signal. We chose 670 nm for thionine and Meldola's blue and 710 nm for toluidine blue where the absorption is red shifted as compared to the other dyes. In addition, the ground-state recovery was monitored in each case at 600 nm. The results are summarized in Figure 1 and Table 2. As shown in Figure 1A(a), the gain signal, probed at 670 nm, indicates that the thionine excited state when bound to [poly(dG-dC)]$_2$ reacts with guanine and is strongly quenched with a single-exponential lifetime of 260 fs. The lifetime of free thionine in the absence of the polynucleotide is more than a factor of 1200 longer, 320 ps,[54,55] which we confirmed by TCSPC measurements. Monitoring the transient bleaching at 600 nm, Figure 1A(b) allows one to follow reformation of the ground state as the reaction products recombine. The signal recovers with a single-exponential lifetime of 760 fs, and this decay will represent the return electron-transfer rate, k_r. Because the measured forward rate is an average of rates to two guanine bases in both the mono- and the polynucleotide studies, the intrinsic rate, k_f, for quenching of the dye will be reduced by a factor of 2; however, this will not affect the return rate because only one base in each complex is reduced. The lifetime for thionine quenched by poly(dG-dT)·poly(dA-dC), where the

(53) Wilhelm, T.; Piel, J.; Riedle, E. *Opt. Lett.* **1997**, *22*, 1494−1496.

(54) Archer, M. D.; Ferreira, M. I. C.; Porter, G.; Tredwell, C. J. *Nouv. J. Chim.* **1977**, *1*, 9−12.

(55) Yamazaki, I.; Tamai, N.; Kume, H.; Tsuchiya, H.; Oba, K. *Rev. Sci. Instrum.* **1985**, *56*, 1187−1194.

Table 2. The Lifetimes for Charge Separation, τ_f, and Recombination, τ_r[a]

dye-nucleotide	τ_f/ps	τ_r/ps	k_f/ps^{-1}	k_r/ps^{-1}	ΔG_f/eV	ΔG_r/eV
thionine-GMP	0.88	1.2	0.57	0.83	−0.42	−1.61
thionine-[poly(dG-dC)]$_2$	0.26	0.76	1.92	1.32	−0.47	−1.56
thionine-poly(dG-dT)·poly(dA-dC)	0.46	2.5	2.17	0.40	−0.47	−1.56
Meldola's blue-GMP	0.45	0.83	1.11	1.20	−0.41	−1.62
toluidine blue-GMP	2.8	5.0	0.18	0.20	−0.26	−1.62
thionine-dAMP	54	≥2500	0.0093	<0.00004	−0.03	−2.06
thionine-[poly(dA-dT)]$_2$	110	≥2500	0.0045	<0.00004	−0.03	−2.06

[a] The intrinsic rate for forward transfer, k_f, is $1/(2\tau_f)$ excepting for the poly(dG-dT)·poly(dA-dC) result where there is only a single guanine in contact with the dye. The driving force of the forward electron-transfer step is $\Delta G_f = E_B - E_D - E_{0-0}$ and the return, $\Delta G_r = E_D - E_B$, where E_B is the oxidation potential of the base (donor), E_D is the reduction potential of the dye (acceptor), and E_{0-0} is the energy of the excited singlet state. E_G is taken to be 1.53 eV in [poly(dG-dC)]$_2$, 1.58 eV in GMP, and E_A 2.03 eV. The Born correction term can be ignored in aqueous solution.

measured rate is an average of reaction with a single guanine only, is 460 fs (not shown), roughly as expected. Similarly, Figure 1B(a) shows that with the mononucleotide, GMP, the excited-state lifetime is 880 fs, and the bleach recovery (b) is 1.2 ps. Meldola's blue is also quenched on the femtosecond time scale by GMP. The excited-state loss, measured at 670 nm, occurs with a single-exponential lifetime of 450 fs, Figure 1C(a) and the ground-state recover with a lifetime of 830 fs (b). For toluidine blue, Figure 1D, the loss of the gain signal occurs with a 3.5 ps lifetime (a), and the ground-state recovery at 600 nm is 5.0 ps (b).

In contrast to guanine, each dye is quenched much more slowly by adenine. Thionine is quenched by dAMP (Figure 1E) with a lifetime of 54 ps (a) and 110 ps by [poly(dA-dT)]$_2$, Figure 1F(a). The recovery of the ground state from the thionine-adenine$^+$ transient species is too slow for us to record accurately. We estimate a decay time of ≥2500 ps for both dAMP and [poly(dA-dT)]$_2$ complexes, Figure 1E(b) and F(b). It is also possible that a small fraction of triplet state contributes to the bleach signal at long time. Fluorescence lifetime measurements confirm the rate of loss of the thionine singlet state, and this avoids any ambiguity as to the origin of each component, since the short decay is also observed in the bleach signal. We also see no evidence in the fluorescence decays for unusually long-lived thionine similar to that reported by Fujimoto et al.[56] for methylene blue in calf-thymus DNA. We note, however, that the high fraction of long-lived fluorescence quoted in that work will be overestimated owing to the limited resolution of the time-correlated, photon counting measurements. The short time decay is ca. 4 ps[25] rather than 25 ps as reported. We would expect that the additional stabilization conferred by the possibility of hydrogen bonding to the exocyclic amino groups in thionine would enhance intercalation as compared with methylene blue and, hence, reduce the fraction of unbound dye.

There is no spectroscopic evidence for binding of thionine to 2′-deoxycytidine-5′-monophosphate, dCMP, or thymidine-5′-monophosphate, dTMP, nor do we observe quenching of the dyes by the pyrimidine bases.

Figure 2 shows the anisotropy decay at 600 nm of thionine bound to [poly(dA-dT)]$_2$. The initial anisotropy at $t = 0$ is 0.2, which decays to a value of 0.09 with a single-exponential lifetime of 200 ps. This is indicative of constrained rotational motion of the dye within the B-DNA type complex. Knowing that reaction occurs with a lifetime of 110 ps in this complex, we can say that rotational reorientation is not limiting and is uncorrelated with electron transfer in the polynucleotide complex. We have also measured a long anisotropy decay of ca. 400 ps for thionine bound to ct-DNA. These observations lead us to a different interpretation of our data than that given by Fiebig et al.[57] for ethidium-ZTP, where rotational motion was proposed to limit the electron-transfer rate.

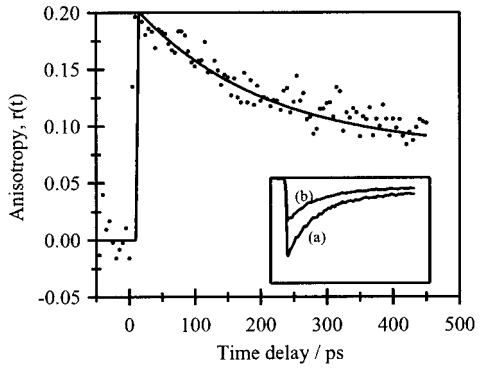

Figure 2. Thionine-[poly(dA-dT)]$_2$ anisotropy at 600 nm. Inset: (a) parallel and (b) orthogonal relative pump−probe polarization signals are shown on the same time scale. The anisotropy decay fits to a single-exponential decay of 200 ps plus background.

2. DNA. Figure 3 shows that thionine is also quenched very efficiently by DNA. However, in contrast to [poly(dG-dC)]$_2$, the decay is not a single exponential, reflecting the range of different intercalation sites. For example, in the case of both calf thymus and salmon testes DNA, approximately 70% of the thionine excited state disappears in 1 ps, the rest with roughly a 30 ps lifetime with a very small fraction of unquenched dye. Thionine is quenched still more efficiently by DNA from micrococcus luteus where almost 90% of the dye is quenched within 1 ps. These data cannot be fit adequately to a simple sum of two exponential decays indicating that the forward electron transfer is more complex. Fitting the early decay to estimate the initial rate of quenching gives 260 fs for reaction with ct- and st-DNA (a similar decay to that for [poly(dG-dC)]$_2$, which has only a slightly higher fraction of guanine) and 206 fs with mc-DNA, indicative of a faster quenching mechanism as the fraction of guanine increases. In the latter case, we believe that quenching by guanine dimers must be considered, and this is discussed below.

Discussion

1. Energetics. Nonadiabatic electron transfer has been explained by Marcus and Sutin[35] who related the rate coefficient, k_0, to the reaction driving force, ΔG, and the reorganization

(56) Fujimoto, B. S.; Clendenning, J. B.; Delrow, J. J.; Heath, P. J.; Schurr, J. M. *J. Phys. Chem.* **1994**, *98*, 6633−6643.

(57) Fiebig, T.; Wan, C.; Kelley, S. O.; Barton, J. K.; Zewail, A. H. *Proc. Natl. Acad. Sci. U.S.A.* **1999**, *96*, 1187−1192.

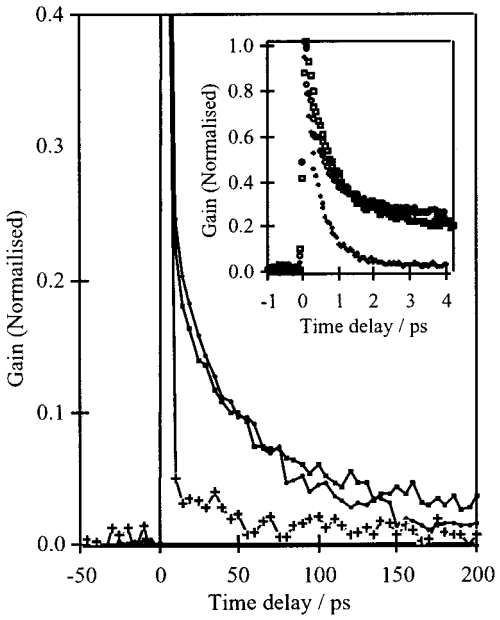

Figure 3. Loss of the thionine singlet state (normalized to +1 immediately after the laser pulse) at 670 nm when bound to calf thymus, ct- (circles), salmon testes, st- (squares), and micrococcus, mc-DNA (crosses). Inset is the same data on a −1 to 4 ps time scale.

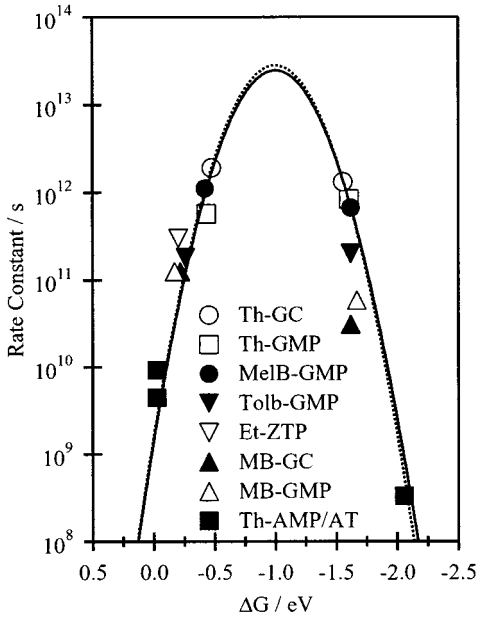

Figure 4. Classical (dashed line) and quantum (solid line) fits to the data given in Table 2. Key: thionine (Th), Meldola's blue (MelB), toluidine blue (TolB), $[poly(dG\text{-}dC)]_2$ (GC), $[poly(dA\text{-}dT)]_2$ (AT). The data for ethidium (Et) are from Fiebig et al.,[57] and methylene blue (MB) from Tuite et al.[27] For the classical fit we used $\lambda = 8070\ cm^{-1}$ and $|V_0| = 330\ cm^{-1}$. For the quantum fit, we used a single promoting mode of 1000 cm^{-1}, a displacement, ΔQ, of 0.05 Å, which gives $|V_0| = 310\ cm^{-1}$ and the reorganization energy $\lambda = 8000\ cm^{-1}$.

energy of the reactants plus solvent, λ, as

$$k_0 = \frac{4\pi^2}{h\sqrt{4\pi\lambda k_B T}}|V_0|^2 \exp(-(\Delta G + \lambda)^2/(4\lambda k_B T)) \quad (2)$$

Ulstrop and Jortner[58] also derived the nonadiabatic rate coefficient, k_0^Q from a quantum viewpoint, using a sum of vibrational promoting modes while treating the solvent classically (so that the vibrational frequencies of the solvent are small in comparison to k_BT). If each promoting mode of frequency, ω_i, has a reduced mass, μ_i, and the displacement between potential surfaces is ΔQ, the rate coefficient, k_0^Q, is

$$k_0^Q = \frac{4\pi^2}{h\sqrt{4\pi\lambda k_B T}}|V_0|^2 F(\Delta G,\lambda,\omega,\Delta Q_i) \quad (3)$$

where F is a complex function of the variables shown.[58]

Despite the ultrafast time scale for some of the electron-transfer reactions, we will analyze our data using these two models, which rely on equilibrium energy gap fluctuations. For the sake of argument, we will assume that the excited-state population rapidly reaches thermal equilibrium, whereas, in reality, thermal equilibration will occur in parallel with electron transfer for the very fastest processes. Excitation at 600 nm was low in S_1, and the bandwidth of the excitation pulses was restricted to ca. 700 cm^{-1} to minimize population of high lying vibrational states.

To estimate accurate values for the reorganization energy and the electronic coupling strength, we require redox potentials for the nucleobases. Steenken and Jovanovic[29] have recently redetermined the oxidation potentials, $E°$, of the nucleosides by pulse radiolysis and give 1.58 V for free guanosine and 2.03 V for adenosine, both of which are considerably higher than those values given previously, 1.33 and 1.73 V, respectively.[59,60] This difference was reported to be the result of experimental complications in the earlier studies. Throughout this paper we have taken GMP to be 1.58 V, G−C to be 1.53 V, and A to be 2.03 V; G−C is slightly lower than the free nucleoside as predicted by calculation.[12] As far as we are aware, there is no data for the distribution of adenine redox potentials with their environments.

Accurate parameters from eq 2 require rate data both close to the maximum on the Marcus curve as well as on longer time scales, and here the fast rates we have determined using thionine are very important. Because time constants greater than a few picoseconds will depend very strongly on redox potential, the fast rates which lie quite close to the curve maximum, where the gradient is smaller, will be the most reliable in determining the coupling and reorganization energies. The solution of eq 2, using the measured forward, k_f, and return, k_r, rates from the thionine reaction with $[poly(dG\text{-}dC)]_2$, gives $\lambda = 8070\ cm^{-1}$ and $|V_0| = 330\ cm^{-1}$ at 298 K. Figure 4 shows the Marcus curve derived from these values, onto which are superimposed the other rate coefficients tabulated in Table 2. We can also extend this argument to previously published data from methylene blue[25] and ethidium-ZTP experiments.[4,57] It may be observed that once again the fit is reasonable, probably because these DNA intercalators, like thionine, are charged and aromatic, and we suggest that they are each stabilized by similar π-stacking interactions. Therefore, to a first approximation we might expect both the electronic coupling energy and the reorganization energy involved to be much the same. Given that both the forward and the return reactions involve charged species in the reactant or product states, it seems reasonable to assume

(58) Ulstrup, J.; Jortner, J. *J. Chem. Phys.* **1975**, *63*, 4385−4368.
(59) Jovanovic, S. V.; Simic, M. G. *J. Phys. Chem.* **1986**, *90*, 974−978.
(60) Jovanovic, S. V.; Simic, M. G. *Biochim. Biophys. Acta* **1989**, *1008*, 39−44.

that the reorganization energy for the forward and reverse reaction is also similar. These two assumptions appear to be supported by our data.

Figure 4 (solid line) shows a fit to the nonadiabatic, quantum model from the equation quoted by Harrison et al.[22] Using a single promoting mode, ω, we obtain the best fit using a very small displacement between reactant and product potentials, ΔQ, of 0.05 Å. The effect of coupling to high-frequency promoting modes is to slow the falloff in rate coefficient with increased driving force in the 'inverted" regime (i.e., when $-\Delta G > \lambda$). This small displacement, ΔQ, means that the fit is relatively insensitive to the frequency of the promoting mode between ca. 100−1000 cm^{-1}. From the best fit, using $\omega = 1000$ cm^{-1}, we again find that the electronic coupling matrix element, V_0, is 310 cm^{-1} and the reorganization energy $\lambda = 8000$ cm^{-1}.

The data we have are well described by this model (i.e., that of a thermally driven reaction from the relaxed excited state of the dye). The rate of vibrational relaxation in the excited state will be similar to the measured rate of forward transfer in [poly(dG-dC)]$_2$. Perhaps more surprising than the fit to the fastest rates is the rapid (parabolic) falloff in rate coefficient in the inverted regime. We might have expected this rate to fall off more gradually from previous measurements of bound donor−acceptor complexes.[22] This observation dictates a fit that is, for the most part, classical, and it follows, therefore, that the coupling to high-frequency vibrations is negligible and also that the possibility of adiabatic electron transfer need not be considered.

2. DNA. If the lifetime of the thionine excited state in DNA were to depend only on the purine base in contact with the dye, then the decay profile would be biexponential decay with lifetimes of <1 ps and ca. 110 ps representing reactions of the dye with either guanine or adenine, that is, in a ratio determined by the GC:AT ratio of the DNA. However, it is clear that our data cannot be explained in this fashion because we see multiexponential behavior, and an increase in initial rate as the fraction of guanine is increased, Figure 3.

It is most insightful to analyze the gain data to simulate the forward electron-transfer reaction rate, since this requires the fewest number of adjustable parameters. First, we consider the short component of the decays and estimate the initial rate for dyes quenched by neighboring guanine. The rate coefficients for quenching by guanine sequences were calculated from the Marcus eq 2, using the reorganization and electronic coupling energies obtained from the polynucleotide studies ($\lambda = 8070$ cm^{-1}, $V_0 = 330$ cm^{-1}). Reduced oxidation potentials of multipurine sequences should result in more rapid quenching of the dye as compared with GC, as these rates are shifted closer to the maximum on the Marcus curve.

The HOMO of 5′-GG and 5′-GA dimers is thought to localize on the 5′-G in a purine stack, thus increasing the probability of oxidation at that position.[46,47] Ab initio molecular orbital studies have been used to estimate the associated redox potentials.[12] Using $E°$ (GT) =1.54 eV, $E°$ (GC) =1.53 eV, $E°$ (GA) =1.38 eV, $E°$ (GG) =1.20 eV, that is, values based on Steenken's[29] potentials corrected according to Saito,[46] gives k_0 (ΔG_{GG}) = 19.4 ps^{-1}, k_0 (ΔG_{GA}) = 2.6 ps^{-1}, k_0 (ΔG_{GC}) = 1.9 ps^{-1}, and k_0 (ΔG_{GT}) = 1.7 ps^{-1}. The average rate for guanine quenching, k_G, will depend on the fraction of G−C pairs in the particular DNA, $k_G = \sum P_{BB} k_0(\Delta G_{BB})$, where P_{BB} is the probability of a guanine base being neighbor to each of the nucleobases, that is, GA, GC, GT, and GG. This average rate we might expect to be an estimate of the early-time signal in the DNA experiments if the ab initio predictions of Sugiyama and Saito[47] of the relative oxidation potentials are accurate. We find, however, that this does not seem to be the case, although the trend is in the right direction; the same conclusion has been drawn in recent experimental[61] and theoretical work.[62] The average calculated initial rate, k_G, in st-DNA is 6.1 ps^{-1} and in mc-DNA is 9.4 ps^{-1}. The initial rate observed in mc-DNA (4.6 ps^{-1}), where a high fraction of GG species should be expected, is also only a little faster than transfer to GC in [poly(dG-dC)]$_2$ (3.8 ps^{-1}) where all dyes have only GC neighbors. If $E°$ (GG) = 1.50 eV, we calculate initial rates in mc-DNA of 4.3 ps^{-1} and 4.0 ps^{-1} in st-DNA, somewhat closer to the experimental values.

The fact that these Marcus parameters predict increased rates for multi-guanine sequences gives us extra confidence in Steenken's higher redox potentials. Reanalysis of the mono- and polynucleotide data, using the lower potentials quoted by Burrows and Muller,[12] yields parameters that predict the opposite trend, that is, a falloff in rate as guanine content increases, since the forward rate from the [poly(dG-dC)]$_2$ experiments appears almost exactly at the maximum on the curve, and the GG redox potential pushes the calculated rate into the "inverted" regime.

Monte Carlo Simulation. The absence of a 110 ps component in the quenching of thionine by DNA (Figure 3) is due to the influence of guanine molecules further away from the dye than the nearest neighbor − these we call the distant guanines. Assuming that the nucleobases are randomly distributed in any DNA and within a superexchange mechanism for electron transfer (with its associated exponential distance dependence), we used a Monte Carlo model to simulate the full decay of the gain signal − the forward electron-transfer process. We require a model that contains at least two adjustable parameters, the redox potential of guanine dimers, so as to fit the initial decay and the distance scaling parameter, β. In addition, Wan et al.[2] observe in their studies of the 2-aminopurine reactions that the rate of electron transfer through pyrimidine bases to distant guanine is reduced as compared with that of adenine intermediates, and we, therefore, require at least a third parameter to account for this behavior.

A single dye molecule was situated in the center of a chain of 10 base pairs as shown in Figure 5, which were assigned at random but weighted according to the known GC:AT ratio of the DNA under study. Each base was assigned a nonradiative rate coefficient according to the polynucleotide studies. Accordingly, single guanine bases have $k_G = 1/(2 \times 260\ fs) - k_f$, where k_f (1/320 ps) is the radiative rate. Multiple guanine sequences are treated such that the 5′G has k_{GG}, calculated from eq 2 using $E°$ (GG), and the others are assumed to be the same as a single guanine, in accordance with Sistare et al.[63] Adenine bases have $k_A = 1/(2 \times 110\ ps) - k_f$, and the rates for C and T transfer, k_{CT}, are assumed to be negligible, that is, slow as compared to the fluorescence lifetime, given that we saw no quenching in the mononucleotide experiments. The distance dependence of the electron transfer was generated from $g_n =$

(61) Lewis, F. D.; Liu, X.; Liu, J.; Hayes, R. T.; Wasielewski, M. R. *J. Am. Chem. Soc.* **2000**, *122*, 12037−12038.
(62) Conwell, E. M.; Basko, D. M. *J. Am. Chem. Soc.* **2001**, *123*, 11441−11445.
(63) Sistare, M. F.; Codden, S. J.; Heimlich, G.; Thorp, H. H. *J. Am. Chem. Soc.* **2000**, *122*, 4742−4749.

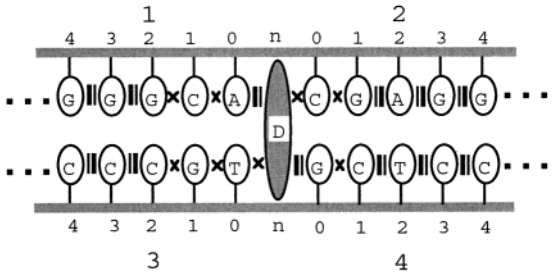

Figure 5. Duplex model for the calculation of the quenching rate of thionine by DNA by a Monte Carlo method. The bases were assigned at random but their number weighted according to the G−C:A−T ratio of the DNA. The four "segments" are labeled 1−4, which are runs of five bases on each strand in either direction from the dye. The dye is assumed to be in van der Waals contact with its neighbors. The coupling of the dye to distant bases depends on the intervening species with a reduction in strength for each break in the sequence. These coupling "defects" are multiplicative and are indicated by crosses between the bases, while the solid black lines indicate efficient coupling between bases of similar energy.

$\exp(-\beta 3.4n)$, where $n = 0-4$ is the number of base pairs away from the dye in each direction, and 3.4 Å is the edge-to-edge unit of separation of the dye from the nearest and subsequent bases. (X-ray crystal data of intercalators in the Brookhaven data bank[64] show that the distance of base to base in DNA is not strongly affected by the intercalating dye.)

Because we have no experimental data for quenching by the pyrimidine bases, we treat them as "spectators" in the electron-transfer process. The binding data of Tuite and Kelly[50] from studies of the absorption spectra of the phenothiazine dyes bound to mono- and polynucleotides show no evidence for interaction with dCMP or dTMP, and, therefore, we expect the predominant π-stacking interaction in DNA to be with the purine bases. Cytosine and thymine will, however, appear as intermediates between the dye and distant guanines, and we must consider the coupling of the dye to these bases through the bridge, taking into account the relative energies of the purine and pyrimidine bases as shown in Figure 6. Superexchange will be most efficient if the energies of the intermediate species are similar, and, therefore, we should not expect a random mixture of bases to make a particular efficient bridge. Some theoretical work exists on the magnitude of the coupling matrix elements,[39,65] which predict that adenine bases are a barrier to electron transfer. These calculations are, however, unable to explain the experimental observations of Wan et al.[2]

The coupling element, $T_{D,A}^{(n)}$, between donor and acceptor, in McConnell's original formulation of the superexchange model,[66,67] appears as a product of individual tunneling integrals, $v_{i,i+1}$, between the degenerate donor and acceptor of energy, $E_{D,A}$, and the n nondegenerate bridging orbitals of energy, E_{B_i}.

$$T_{D,A}^{(n)} = \prod_{i=1}^{n} \frac{v_{i,i+1}}{E_{D,A} - E_{B_{i+1}}} \tag{4}$$

We, therefore, introduce a coupling parameter, $c = 1$, between adjacent, similar bases (either purine or pyrimidine), but $c \leq 1$ between dissimilar bases indicating a region of reduced coupling in the bridge. This is shown in Figure 5 where the crosses are indicative of the coupling "defects" in the strands. Consequently, the total coupling through the bridge in our model will be a product of these parameters; $c < 1$ reduces $|V_0|^2$ in eq 2 and hence also the rate coefficient, k_0, when the bridge contains a mixture of A with C or T. The pyrimidine bases thus shield the dye from distant purines.

We divide the total quenching rate coefficient into the sum of four parts, which correspond to the four "segments" labeled 1−4 in Figure 5, that is, both toward and away from the 5′ end in a single strand and in its complement. The total quenching rate coefficient, k_{seg}, in each of these segments is simply the sum of the rate coefficients for quenching by each individual base at a distance of $n \times 3.4$ Å,

$$k_{seg} = \left(\sum_{n=0}^{m} (k_n g_n \prod_{0}^{n} c_n)\right) \tag{5}$$

where k_n is the nonradiative rate for each base, k_G, k_{GG}, k_A, or k_{CT} at position n, m is the furthest base from the dye in the segment (i.e., when $n = 4$), g_n is the distance scaling factor, $\exp(-\beta 3.4n)$, and c_n are the coupling parameters. The total decay was then calculated according to eq 6,

$$I(t) = \frac{1}{i}\sum_{i} \exp(-t[k_f + \sum_{seg=1}^{4} k_{seg}]) \tag{6}$$

for i repeated calculations, typically 50 000.

While all three parameters, β, $E°$ (GG), and c, describe the data in detail, for the purposes of discussion the decays can be divided in three parts. The initial decay is primarily due to the average rate of guanine quenching by nearest neighbors in the DNA, which will depend on the relative redox potentials and concentrations of the guanine species present, as discussed above. A slower component, the 30 ps lifetime in the st-DNA data, is determined largely by β and is due to transfer to distant guanine, while the reduced coupling owing to the bridge defects, c, influences the remainder of the long-time component of the decay. We obtained the best global fit, shown in Figure 7, to the st-DNA and mc-DNA data using a least-squares method, calculating a weighted, reduced χ^2 for both decays simultaneously. β was varied from 0.5 to 1.0, c from 0.05 to 1, and $E°$ (GG) from 1.45 to 1.55. This analysis yields the three parameters: $\beta = 0.8 \pm 0.1$ Å^{-1}, the redox potential $E°$ (GG) is 1.50 ± 0.01 eV, significantly larger than that predicted by the molecular orbital calculations, and the coupling parameter, c, is 0.20 ± 0.05. The error on the redox potential is small since this appears in the exponential in the Marcus equation and is, therefore, relatively sensitive. We do not believe $E°$ (GA) is significantly different from $E°$ (GC) for the same reason. The errors given represent the precision within the limits of the redox potentials we have used rather than the accuracy, which will be dictated by the limits of Steenken's measurements.[29] Our model takes account of both the fast and the slower components in the decay over 3 orders of magnitude in time and intensity while returning a β value that is consistent with the results on the small and well-defined oligomers.[2,3,68]

(64) Kielkopf, C. L.; Erkkila, K. E.; Hudson, B. P.; Barton, J. K.; Rees, D. C. *Nat. Struct. Biol.* **2000**, *7*, 117−121.
(65) Voityuk, A. A.; Jortner, J.; Bixon, M.; Rosch, N. *J. Chem. Phys.* **2001**, *114*, 5614−5620.
(66) McConnell, H. M. *J. Chem. Phys.* **1961**, *35*, 508.
(67) Todd, M. D.; Nitzan, A.; Ratner, M. A. *J. Phys. Chem.* **1993**, *97*, 29−33.
(68) Lewis, F. D.; Wu, T.; Zhang, Y.; Letsinger, R. L.; Greenfield, S. R.; Wasielewski, M. R. *Science* **1997**, *277*, 673−676.

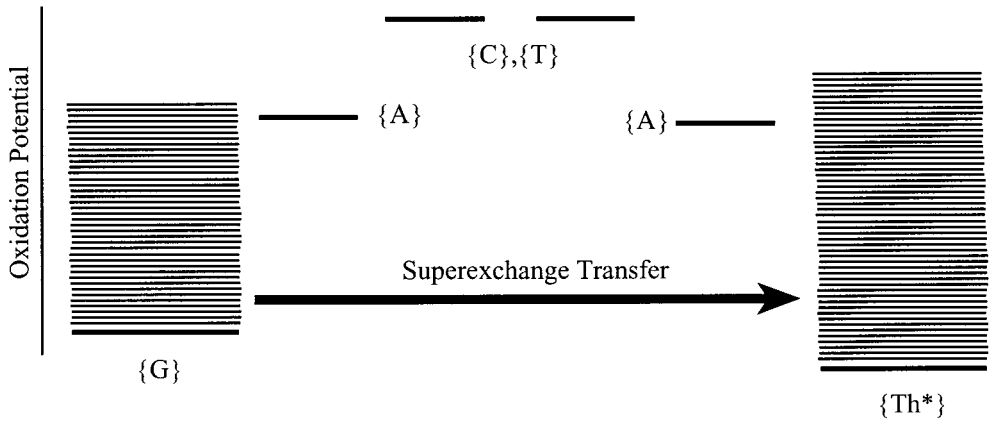

Figure 6. Electron transfer via superexchange from a nucleobase to the thionine excited state. If a bridging base is higher in energy (here C or T vs A), efficient coupling through the vibronic manifolds of an inhomogeneous sequence will be reduced in comparison with that in a bridge consisting only of A.

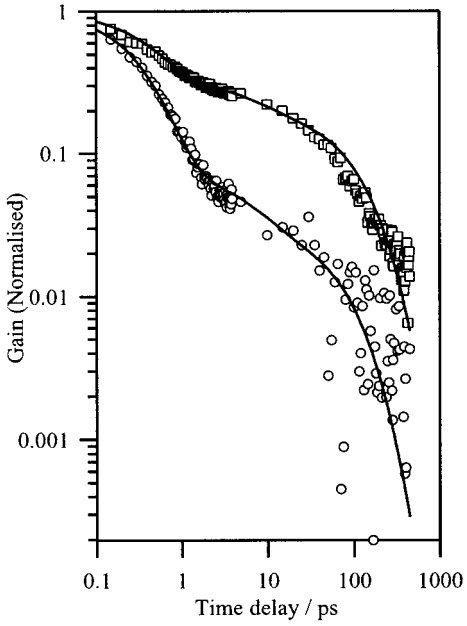

Figure 7. Data and results of a Monte Carlo simulation of the forward electron-transfer rates in DNA. We show global fits to the DNA from salmon testes (41.2% G−C, squares) and to DNA from micrococcus luteus (72% G−C, circles) using our reduced coupling model. β, the electron-transfer distance parameter, is 0.8 ± 0.1 Å^{-1}, and the coupling parameter is 0.20 ± 0.05. The noise in the mc-DNA data is due to the small amount of DNA we had available. The data and fit are scaled to +1 at $t = 0$ ps.

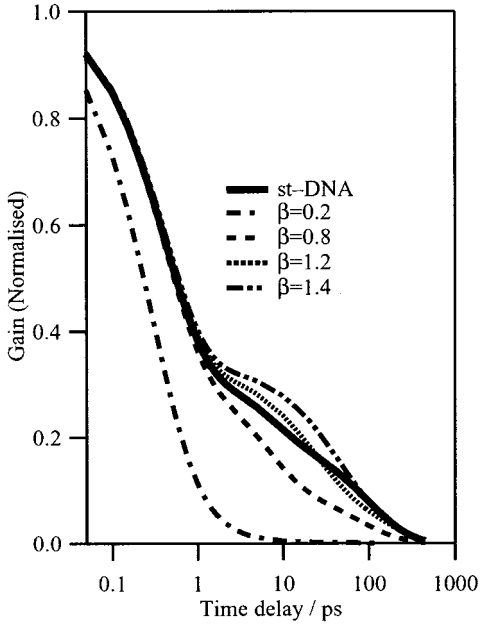

Figure 8. st-DNA vs β in the absence of the coupling defect parameter ($c = 1$). The thickness of the solid line is indicative of the signal/noise ratio of the data. Note the linear-log scale − this best shows deviations of the fit in the region of the turnover from fast to slower quenching. The high β values also underestimate the fraction of short decay, which is not so clear on this scale.

Because the product of coupling integrals in eq 4 leads to an exponential distance dependence, our model can be thought of as an electron-transfer process that has many values of β depending on the exact structure of the bridge. For example, the reduced rate to a guanine at $n = 1$ through a single C or T base falls off markedly, β is ca. 1.75 Å^{-1}. We observe that electron transfer (or hole transfer) into DNA segments is less efficient when the superexchange bridge is composed of mixed bases, and, in this respect, the pyrimidine bases can be thought to act much more like insulators within the DNA chain.

As a test of our model, Figure 8 shows the effect of removing the coupling parameter from the model, that is, $c = 1$, as compared to the st-DNA data, such that bridge defects do not shield distant purines from the dye. We have made a linear-log plot in this instance, which emphasizes the shape of the decay in the region of the changeover from nearest neighbor quenching to distant quenching. Varying β systematically from 0.2 to 1.4 Å^{-1} while holding $c = 1$ and E° (GG) = 1.5 eV produces significantly poorer fits than those shown in Figure 7.

Table 3. Calculated Quenching Rates of Thionine by Guanine, for Nearest Neighbor and Next Nearest Neighbor Species[a]

sequence	E° (G)/eV	Πc_n	rate/ps^{-1}
dye−G	1.53	1	1.9
dye−(G−G)	1.50	1	2.6
dye−A−G	1.53	1	0.13
dye−C/T−G	1.53	0.04	0.005
dye−space−G	1.53	*b*	0.009

[a] $\beta = 0.8$; G is guanine adjacent to C, T, or A, and (G−G) is a guanine duplex. [b] Shown for comparison is the direct (nonsuperexchange) rate through space, 3.4 Å, assuming a typical β of 1.4 Å^{-1}.

Table 3 gives the calculated quenching rate of thionine by a single neighboring guanine, k_G (1.9 ps^{-1}), or guanine dimer, k_{GG} (2.6 ps^{-1}). If the dimers are only ca. 30 mV lower in oxidation potential than other guanine species, the quenching rate increases by a factor of 1.3. Also given is the quenching

rate for thionine separated from a guanine base by a single adenine (0.13 ps^{-1}) as compared with coupling through one of the pyrimidines (0.005 ps^{-1}) a factor of 26 smaller and comparable to direct transfer (nonsuperexchange) over 3.4 Å assuming a β of 1.4 $Å^{-1}$, that is, more typical of a "normal" environment. For the sake of clarity, we did not include direct transfer in the model, but the small fraction of extra quenching by the direct route would have the effect of reducing c a little further.

Our model clearly predicts that there is some degree of restriction on the pathways to electron-transfer products due to the high energy of the pyrimidine bases. This also leads us to the conclusion that interstrand coupling through the hydrogen bonds must be negligible as compared with coupling through the π-stack. If cross-strand electron transfer were possible, the electron or hole might be thought to "zigzag" between segments, finding the nearest guanine, and again this would result in overly rapid quenching. This conclusion is in broad agreement with the observations of Lewis and co-workers[3] that the electron does not cross strands on a picosecond time scale.

Conclusions

Electron transfer between charged, intercalating dyes and DNA has been described using the classical Marcus description as well as a nonadiabatic, quantum model. We estimate that the electronic coupling energy, $|V_0|$, is ca. 330 cm^{-1}, and the reorganization energy is ca. 8070 cm^{-1} for both forward and reverse reactions. The coupling strength is a little large, relative to k_BT, to be strictly in the nonadiabatic limit, and the fastest rates will occur in competition with vibrational relaxation in the excited state, but, nevertheless, we find the Marcus equation able to fit these data over >4 orders of magnitude in rate. We also observe that rotational reorientation of the dyes is uncorrelated with electron transfer.

We bring together recent observations from synthetic DNA oligomers and show that the results are general to natural DNAs. We find a distance dependence ($\beta = 0.8 \pm 0.1$ $Å^{-1}$) which is similar to values obtained by Lewis et al.[68] and, independently, by Wan.[2] Our model requires a higher redox potential for guanine dimers than has been predicted previously from ab initio calculations,[46,47] but it is in line with other recent reports.[61,62] The predictions of lower redox potentials for the guanine dimers were based on the observation that oxidative strand cleavage often occurs at multi-guanine stacks. Our results would not necessarily contradict these experimental reports; we would merely conclude that those processes do not occur on a picosecond time scale. Once an isolated hole is present in a DNA strand, it may of course migrate as described, for example, by Giese[69] who reports the possibility of trapping at multi-guanine sites.

We also infer that the high energy of the pyrimidine bases significantly affects the efficiency of electron transfer in DNA. The effects of inhomogeneity via site and energy disorder on electron-transfer rates in real DNA, as compared to the much better defined oligomers used in the studies of Lewis and of Wan, do not appear to influence the measured β very strongly; that is, the primary limit to the rate of electron transfer in superexchange is the energy difference between adenine and the pyrimidine bases. We also infer that the superexchange mechanism is not enhanced by the hydrogen bonding network but only by the π-stack.

Acknowledgment. G.D.R. is a Royal Society University Research Fellow and thanks The Royal Society for its generous financial support. We also acknowledge the award of EPSRC studentships to D.J.W. and M.A.D. J.M.K. acknowledges the Berkeley Fellowship from Trinity College Dublin. D.A.T. is a SCI Messel Scholar.

JA0172363

(69) Giese, B. *Acc. Chem. Res.* **2000**, *33*, 631−636.